Allometry in an eco-evolutionary network model

ABERNETHY, Gavin <http://orcid.org/0000-0001-6983-6349>

Allometry in an eco-evolutionary network model

Gavin M. Abernethy[a]

[a]*Department of Engineering and Mathematics, Sheffield Hallam University, UK*

Keywords: Eco-evolutionary model; Food webs; Allometric scaling; Spatial model

Abstract

An eco-evolutionary food web model is modified to incorporate a body-size trait, enabling a framework for non-uniform mortality and ecological efficiency between species. Evolved communities feature increased connectance, with according benefits to community robustness, and persistent top predators but reduced omnivory and food chain lengths. Body-size maintains a strong positive correlation to trophic level, but does not correlate to an individual species' contribution to network stability. A spatially-explicit extension of the model assembles large metacommunities with distinct distributions of body-size amongst local food webs.

1. Introduction

The simplest description of an ecosystem is to arrange the food web into a trophic level structure indicating energy transfer. This implies a hierarchical ordering of species, and so many food web models have been based on assigning some "niche" value to each species that will determine their feeding relations. A natural question is if this value corresponds to a specific morpohological or physiological property, such as body mass [WL87] which is known to influence animal metabolism [Hem60, BGA+04]. A major empirical collaboration in the 2000's confirmed that 80% of recorded predator-prey interactions are between smaller prey and larger predators [BJB+06], with the ratio varying over several orders of magnitude according to habitat and organism type. In their bioenergetic approach, which has become the paradigm for many subsequent population dynamics studies, Yodzis and Innes related the metabolic rates, body-size, and classifications of organisms (for example, endotherms vs. ectotherms) [YI92]. Rates of metabolism (usually implemented as a variable ecological efficiency), respiration (as natural death rate) and equilibrium biomass density (see the metabolic theory of ecology [BGA+04]) may follow a law of scaling with adult body mass x in proportion to $x^{0.75}$ (or $x^{-0.25}$ per unit mass) [Pet83], although alternative relations such as $x^{2/3}$ have also been proposed [WS03]. This type of relationship is known as allometric scaling.

This theory that body-size could provide an organising principle for food webs formed the basis of the eco-evolutionary model proposed by Loeuille and Loreau [LL05], which connected the one-dimensional hierarchical arrangement of species in the static cascade [CPYS93] and niche [WM00] models of food web networks with a body mass value subject to mutation and evolutionary selection. This was followed by a study of ecological dynamics imposed on niche model structures [GD08], where metabolism and natural death rate scaled with the niche value associated with the organism's adult body mass. Subsequently, a modified version of the niche model directly equated the assigned niche value with the organism's body-size [WAP10]. Other authors have similarly imposed body-masses and allometrically-determined feeding relationships on model networks [BDM+09]. By correlating the effects of species deletion on the population sizes of each of the remaining species against many food web parameters, they demonstrated that only the biomasses and body-sizes of two species were required for a reasonable prediction of the effect of deleting one on the other. This evidences the organisational power of body mass, and gives some hope that, with regard to conservation, the response of food webs to perturbation may yet be predictable despite their complex nature. On the role of allometry in network stability, some studies have evidenced that food web structures incorporating body-size structure can attain positive stability-complexity relationships [CRGB08, BWM06, KHDG10], or have increased stability in the sense of community robustness [KGD09]. Heckmann et al [HDBG12] combined adaptive foraging and allometric scaling of metabolic rates in model food webs, demonstrating that allometric scaling can have a stabilising influence if the food web structure ensures predators are consistently larger than their prey. Moreover, through its combination with adaptive foraging it is possible for this predator-prey size-structure to emerge from an initially random network as an evolutionary result of dynamic models seeking stable webs.

Email address: G.M.abernethy@shu.ac.uk (Gavin M. Abernethy)

In previous work, we have refined [AMG19a] and extended [AMG19b] the Webworld eco-evolutionary food web model [CHM98, DHM01], which simulates the assembly and maintenance of a community of interacting species from an initial species and resource, using discrete traits to distinguish species and determine their feeding relationships. This model has been successful at constructing complex food webs with realistic properties and has been given considerable attention [DMQ04, QHM05a, QHM02, QHM05b, LM08a, LM08b, McK04], however some weaknesses remain. First, it is not obvious how ecological efficiency and mortality rate should be varied between species, and so these are universal constants in all previous iterations of the model. Second, while co-evolution of species whose role and trophic position are emergent properties is a major advantage of eco-evolutionary models, it does not seem realistic that the communities generated are essentially arbitrary. The advantages or disadvantages of a particular trait are defined completely in terms of the other species that exist in the food web, such that a species which is basal in one environment could become a top predator if placed in a different habitat where higher-level species shared many traits with the previous resource.

In this work we have combined the principles of allometric scaling discussed above with the Webworld model. We will study the impact this has on the food webs constructed by the model, and investigate the role of body-size in a spatial extension of the model to multiple patches.

2. Developing an allometric Webworld model

2.1. Background and intent

The base description of the Webworld model is given by Drossel et al [DHM01]. Some changes were made in our recent study [AMG19a], in particular the method of choosing a parent during the speciation process is now proportional to total species biomass which was also equivalent to population size. This was subsequently extended to a spatially-explicit metacommunity model [AMG19b].

In this model, species are defined by a list of discrete traits that they possess, which determine their predator-prey relationships. Other researchers have used a continuous body-size trait to define species and govern their interactions. In the model by Loeuille and Loreau [LL05], species experience competition with those within a window of similar body-size, and prefer to feed on species whose body-size lies within a window generally lower than that of the predator. They allowed body-size to be subject to mutation when a child species was created. This model was altered by Brännström et al [BLLD11] to account for relative rather than absolute differences in body-size between potential predator-prey pairs, so as to promote ecosystems with body-sizes ranging over several orders of magnitude. Loeuille and Loreau's work was also extended by Allhoff and Drossel [ARR+15] to allow the position and size of the feeding windows on the body-size axis to also be subject to mutation, and this model with three evolving properties was further extended to a spatially-explicit version [BDA17, RJDA18].

In this paper, we have incorporated the implementation of body-size in Brännström et al's version of the Loeuille-Loreau model [BLLD11] to our existing version of the Webworld model [AMG19a], so that in addition to the usual ten discrete traits, each species also has a body-size drawn from a continuous range. This allows us to distinguish between biomass and population size, utilise a non-uniform mortality rate (thus addressing one of the weaknesses of Webworld), and introduce a hierarchy to the species which can give us a sense of the maturity of the ecosystem. Species will no longer be essentially arbitrary with an unrealistic degree of flexibility, and instead this should enable diversity of species to exist within broad trophic bands. We will investigate the implications of making this change on the non-spatial model, and the evolution of the distribution of body-sizes in the community. We will also consider the effect of this alteration on the stability of the networks generated by the model, and the consequences of allometry for the spatial extension of the model.

2.2. Model description

We here provide a comprehensive description of the model, which primarily consists of three nested stages: the evolutionary, ecological, and foraging loops. An outline of the broad steps of this process is illustrated in a schematic (Figure 1).

Initialisation

To begin a simulation, the Webworld model generates a 500×500 antisymmetric trait matrix β with scores drawn from a Gaussian distribution between zero and one. In every patch, a unique resource species with size $s_0 = 1$ is then created by assigning it ten random non-repeating traits, and finally one initial non-resource species with population size 1.0 and body-size $s_1 = e$ is generated that can feed on the resource in the first patch.

Each species i has a local population in a given patch denoted by N_i, and its body-size s_i is converted to a logarithmic scale with $r_i = \ln(s_i)$.

The simulations in this paper will then construct food webs over either 110,000 or 500,000 evolutionary timesteps.

Evolutionary timestep

Each of these consists of iterating the ecological loop described below until either a steady state (fixed point or cycle up to period 10) is achieved within a tolerance of 0.1 for all local populations, or a maximum of 100,000 ecological timesteps have been performed. After either of these conditions has been met, a speciation event occurs. Thus, an evolutionary timestep is defined simply as the amount of time between two speciation events, and does not represent a specific amount of real time in years.

During a speciation event, a non-resource species and local population is selected with probability proportional to the population size. Then a child species with the minimum population size of 1.0 is introduced, and the parent population is reduced by 1.0, in the same patch. The child retains 9 of the parents' 10 traits, while one trait is

randomly selected and exchanged for a random trait other than the 9 currently possessed. If the new trait set matches another species that already exists in the metacommunity (even if the body-sizes are different), then a population size of 1.0 is simply exchanged between the parent and this species in the patch where mutation is occurring. Assuming that a different trait has been selected and a new species therefore created, the child's body-size is chosen from a uniform distribution within a factor of [0.8, 1.2] of the parent's body-size. Note that in spatial models, patches with very low diversity are less likely to be the location of a speciation if they have low total populations, however this mechanism reduces the potential disparity between disconnected patches compared to choosing parental species with equal probability (where it is possible for most mutations to only occur in a single patch).

Ecological timestep

An ecological timestep consists of the following process for (i) foraging, (ii) feeding and reproduction for each species, followed by (iii) movement of populations in a spatial model, and finally (iv) resetting the populations of the resources.

(i) If it is the first ecological timestep following either a mutation event, or the extinction of a species, we alternately iterate the "foraging timestep" between the following two steps (a) and (b), until either a fixed point is reached with tolerance 0.01 for all foraging efforts $f_{i,j}$, or a maximum of 1,000,000 foraging timesteps have been performed. For all subsequent ecological timesteps, they are each updated precisely once, as individuals incrementally adjust their feeding strategy in response to the outcome of the previous ecological timestep. This is a change to previous versions of the Webworld model, in order to (i) increase the speed of the simulation by removing the third nested loop in most circumstances, and (ii) create a more realistic model where predator behaviour is a response to circumstances experienced, rather than an optimal strategy decided with perfect information (and agreement in a sense) of the future behaviour of all species in the ecosystem.

Foraging timestep

(a) For each predator i, distribute the foraging efforts on prey j (if it is the first foraging timestep of the first ecological timestep, distribute them equally amongst possible prey), according to the equation:

$$f_{i,j} = \frac{g_{i,j}}{\sum_{k \in K_i} g_{i,k}} \tag{1}$$

where K_i is the set of species who are potential prey of species i (that is, $S_{i,j} > 0$ where S is the matrix of feeding scores described below). As described in [DHM01], if predator i has the potential to feed upon prey j but chooses not to do so, maintain the effort at a minimum of $f_{i,j} = 10^{-6}$ for computational reasons.

(b) For each predator i, update their ratio-dependent functional responses $g_{i,j}$ for each prey j according to the formula developed in [DHM01]:

$$g_{i,j} = \frac{S_{i,j} f_{i,j} N_j}{b N_j + \sum_{k \in P_j} \alpha_{i,k} S_{k,j} f_{k,j} N_k}, \tag{2}$$

where:

- $b = 0.005$ is a saturation parameter which scales feeding scores in the simulation. This parameter value is chosen to follow previous work [DHM01].
- $S_{i,j}$ is the non-negative trait score of i against j. It is calculated as an average of the scores of i's traits against j's traits, and this is then scaled by the body-size feeding kernel, which favours feeding on species that are approximately one order of magnitude smaller in size:

$$S_{i,j} = \max\left\{0, \frac{1}{10} \sum_{m=1}^{10} \sum_{n=1}^{10} \beta_{u_m, v_n} \times M_\gamma \gamma(r_i - r_j)\right\}, \tag{3}$$

where u_m is the m^{th} trait of species i, v_n is the n^{th} trait of species j, β_{u_m,v_n} is the score of trait u_m against trait v_n, and the feeding function of species i on j obeys:

$$\gamma(r_i - r_j) = \frac{1}{\sigma_\gamma \sqrt{2\pi}} \exp\left(\frac{-(r_i - r_j - \mu)^2}{2\sigma_\gamma^2}\right) \tag{4}$$

Following previous authors [BLLD11], we set $\mu = 3$, $M_\gamma = 10$, and $\sigma_\gamma = 1.5$. Therefore in this implementation, if the prey j is of the ideal body-size for a predator i (that is, $s_i = s_j \exp(3)$), the

feeding score $S_{i,j}$ can be raised by a maximum factor of $10(1.5\sqrt{2\pi})^{-1} \approx 2.66$ relative to the non-allometric version of the model, while prey with non-optimal bodysize will have reduced feeding scores. For example, a predator-prey score between two species of identical size will be reduced by a factor of $10(1.5\sqrt{2\pi})^{-1} \times \exp(-9/(2 \times 1.5^2)) \approx 0.36$. Thus we emphasise that this has *not* imposed a strict ordering that species *must* be restricted to feeding on prey of lower body-size, but they will certainly have a preference to do so.

- P_j is the set of species who are predators of j.
- $\alpha_{i,k}$ is the symmetric competition strength of i against k. This is calculated using:

$$\alpha_{i,k} = c + (1-c) \times q_{i,k} \times M_\alpha \alpha(r_i - r_j) \tag{5}$$

where $c = 0.6$ is the competition parameter describing how the strength of interspecific competition tails off between biologically-distinct species. This value is within the a range investigated in prior work [DHM01, AMG19a] that gives rise to large, complex food web networks. $q_{i,k}$ is the fraction of traits of species i that are also possessed by species k, and:

$$\alpha(r_i - r_j) = \frac{1}{\sigma_K \sqrt{2\pi}} \exp\left(\frac{-(r_i - r_j)^2}{2\sigma_K^2}\right) \tag{6}$$

with $M_\alpha = 1$ and $\sigma_K = 0.6$ [BLLD11].

(ii) Update the local populations N_i, as a result of feeding and reproduction, using the Euler method with step size 0.1, according to the balance equation:

$$\frac{\mathrm{d}N_i}{\mathrm{d}t} = -d_0 \, \mathrm{e}^{-qr_i} \, N_i + \lambda \frac{N_i}{s_i} \sum_{j=0}^{n} g_{i,j} s_j - \sum_{k=1}^{n} N_k g_{k,i} \tag{7}$$

where the terms on the right-hand-side represent species i's natural death rate in the absence of predators, population gain due to predation and population loss due to being predated upon. Here, the mortality rate is now scaled allometrically. This has the effect that larger species will have longer lifespans and thus can persist despite the greater amount of biomass required per new individual. In particular, $q = 0.25$ and we choose $d_0 = 2$ (rather than 1 as in [BLLD11]), so that the death rate of the initial species i is approximately $-1.2 \times N_i$ and thus on the same order as in the original model. λ is the ecological efficiency parameter that controls the fraction of consumed prey biomass that contributes to new predator biomass. This is often chosen as 0.1 [Pim82], but to offset the reduced trophic levels caused by the allometric scaling, we increase it to 0.3 for this version of the model.

If the local population N_i of species i falls below the threshold value of 1.0 in all patches, the species is considered extinct and removed from the network. As described above, at the next ecological timestep the foraging equations (1) and (2) will be iterated repeatedly to allow remaining species to re-orient themselves to the new configuration of prey.

(iii) In spatial versions of the model, movement now takes place between adjacent patches. The population of species i in patch (x, y) is then given by:

$$N_{i,x,y} \mapsto N_{i,x,y} + \sum_{j=1}^{x_{max}} \sum_{k=1}^{y_{max}} \delta_{j,k,x,y} \mu_{i,j,k,x,y} N_{i,j,k} - \sum_{j=1}^{x_{max}} \sum_{k=1}^{y_{max}} \delta_{x,y,j,k} \mu_{i,x,y,j,k} N_{i,x,y} \tag{8}$$

where $\delta_{j,k,x,y} = 1$ if the patches (j, k) and (x, y) are adjacent (not diagonally) and distinct, and zero otherwise, and $\mu_{i,j,k,x,y}$ denotes the fraction of the local population of species i in patch (j, k) that migrates to patch (x, y) at this time step. This depends on the choice of ruleset for migration, discussed below, but is always a function of the population of species i that currently exists in patch (j, k). We also implement a minimum movement threshold of one whole individual, so that if $\mu_{i,j,k,x,y}$ is less than 1.0 we set it to zero.

In Section 4, two sets of rules for population movement will be compared. In both cases, individuals only emigrate from the patch they currently occupy in response to a decrease in the local population since the previous ecological timestep - whether that is because of predation or a lack of food. In previous studies, this rule could successfully assemble a metacommunity with different arrangements of species in each patch [AMG19b]. In one variant, the rate of movement is also scaled allometrically, so that larger species are able to move in greater quantities, as has been employed in other studies [BDA17]. However, since larger species will be able to sustain

fewer individuals, there is potential for an evolutionary trade-off between the advantages of greater range and mobility and the disadvantage of lower population sizes for large-bodied species. Writing the local population of species i in patch (j,k) at the t^{th} ecological timestep as $N^t_{i,j,k}$, this rule can be expressed as:

$$\mu_{i,j,k,x,y} = \begin{cases} 0.3\frac{s_i}{s_0} \times \frac{N^{t-1}_{i,j,k} - N^t_{i,j,k}}{N^{t-1}_{i,j,k}} \times D^{-1}_{(j,k)}, & \text{if } N^{t-1}_{i,j,k} > N^t_{i,j,k} \\ 0 & \text{otherwise} \end{cases} \tag{9}$$

where $s_0 = 1$ is the resource body-size and $D_{(j,k)}$ is the number of available patches adjacent to patch (j,k) so that emigration is independent of the patch's connectedness.

The second, non-allometric variant to be compared is:

$$\mu_{i,j,k,x,y} = \begin{cases} \frac{N^{t-1}_{i,j,k} - N^t_{i,j,k}}{N^{t-1}_{i,j,k}} \times D^{-1}_{(j,k)}, & \text{if } N^{t-1}_{i,j,k} > N^t_{i,j,k} \\ 0 & \text{otherwise} \end{cases} \tag{10}$$

The scaling constant 0.3 in equation (9) is chosen so that these two rules will yield migration rates of comparable order for the initial non-resource species, who have body-size e.

(iv) As the final step of a single ecological timestep, the local populations of the resource species are replenished to their parameter value, which is set at $\lambda^{-1} \times 100,000$, so that the resource is never permanently depleted.

2.3. Data collection

The data collected during and at the end of simulations includes the following:

- Population, biomass and body-size of each species.
- Diversity: the number of species present in the ecosystem, including the resource.
- The fraction of the number of species in the ensemble classified as *Basal* (feeds directly upon the reason, although not necessarily exclusively), *Top* (not basal, and with no predators), and *Intermediate* (all other species).
- Trophic levels. We employ two measures of the trophic level of a species:
  - Shortest-chain trophic level (SCTL). This is an integer value giving the shortest path from the species to the resource, so a species that feeds directly on the resource has shortest-chain trophic level of 1 even if it also devotes some effort to predating other species.
  - Prey-averaged trophic level (PATL). This measure of trophic level considers the whole of a species' diet, weighted according to the proportion of feeding efforts allocated.

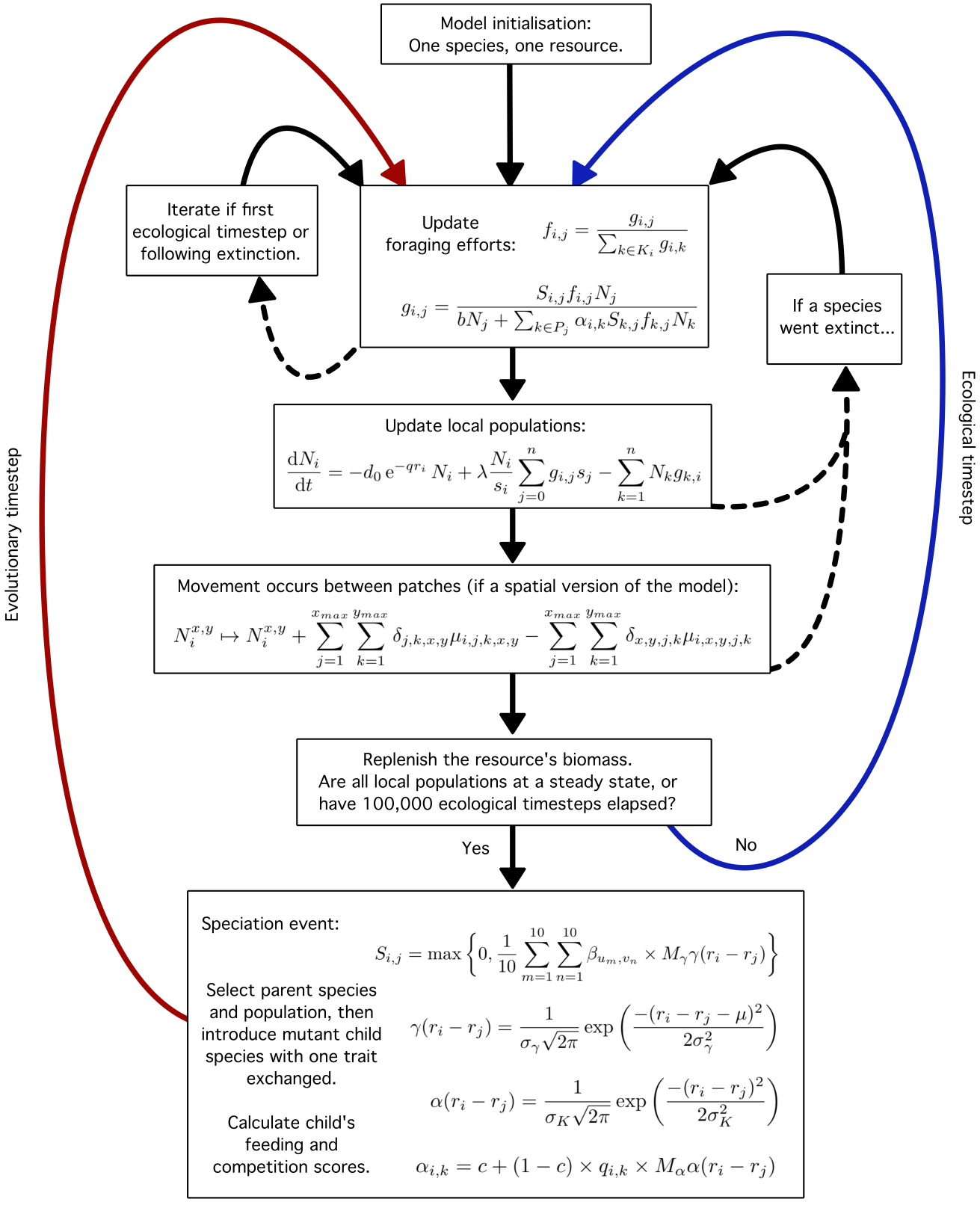

Figure 1: Outline of the iteration of the Webworld model. Dashed lines indicate conditional processes. The primary internal loop (an ecological timestep) is coloured blue, whilst red denotes the external loop (an evolutionary timestep)

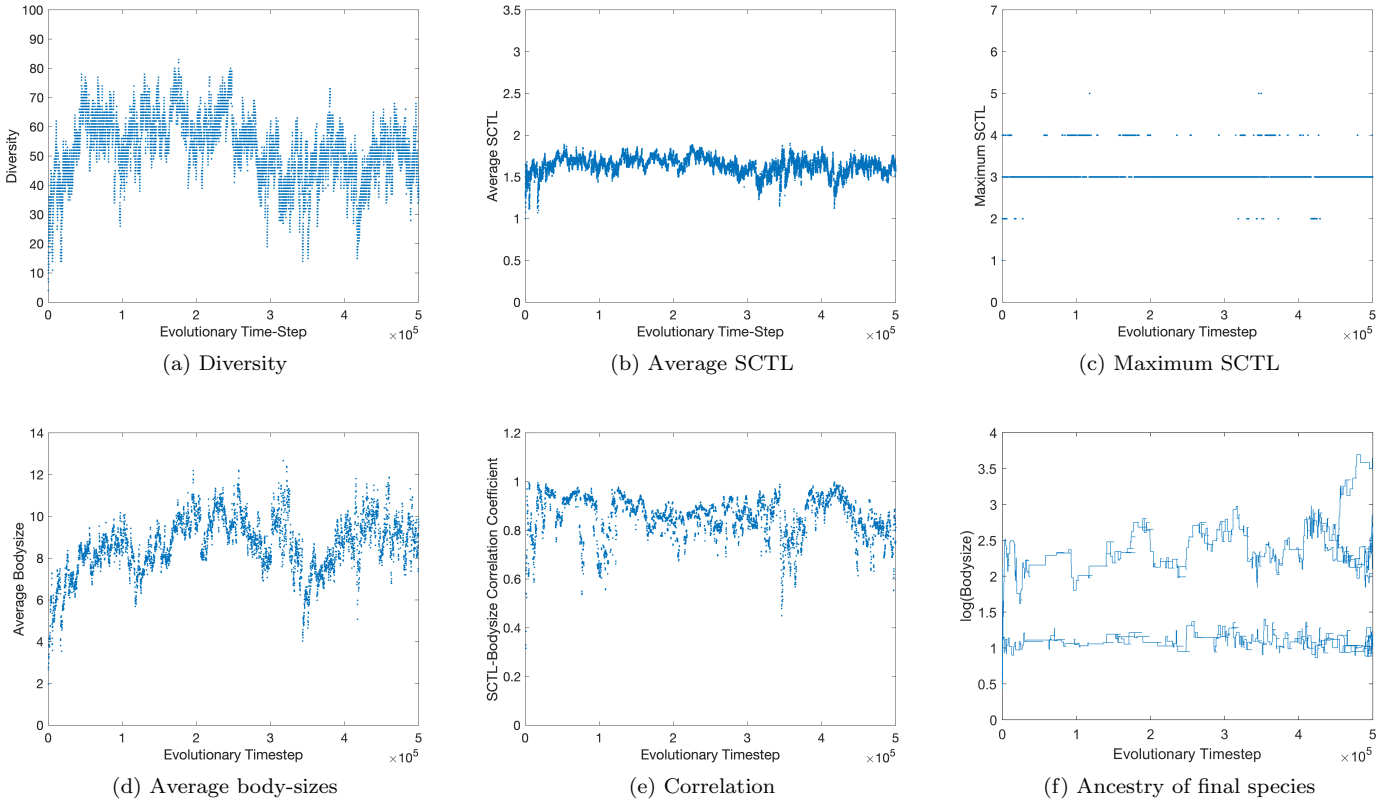

(a) Diversity (b) Average SCTL (c) Maximum SCTL

(d) Average body-sizes (e) Correlation (f) Ancestry of final species

Figure 2: Timeseries of properties in the allometric model

3. Single patch simulations

We begin by modelling the development of a food web in a single patch, with no movement or spatial element. All simulations have a length of 500,000 evolutionary timesteps, and the parameters and initial conditions are as described in Section 2 unless stated otherwise.

3.1. Time-series of one allometric simulation

Consider the timeseries of properties over a single simulation of the allometric version of the model. The diversity of the ecosystem follows a pattern of peaks and troughs (Figure 2(a)), similar to those produced by the standard Webworld model [AMG19a]. When many species are present, and the average body-size is large, there is a very strong correlation between body-size and trophic position (Figure 2(e)). This correlation lowered during a period around 350,000 evolutionary timesteps when both diversity and the average body-size of the species dipped significantly. From Figure 2(c), this was due to a wave of extinctions at higher trophic levels. As a result, all species occupied the first or second trophic levels, regardless of variation in body-size, and so the scope for a strong correlation was reduced. In Figure 2(f), we illustrate the evolution of body-sizes (on a logarithmic scale) and parent-child relationships of the direct ancestors of any species which exists in the food web at the end of the simulation. There is a branching point very early in the simulation that ultimately gives rise to all species with body-size greater than exp(1.5), who will generally occupy the second and third trophic levels. This evolutionary branch remains separated from the species with body-size approximately equal to e who compete directly for the resource. Note that the tree appears denser as the number of evolutionary time-steps approaches 500,000, as many of these younger species may eventually go extinct if the simulation were allowed to continue.

The final food web constructed by this simulation is shown in Figure 3.

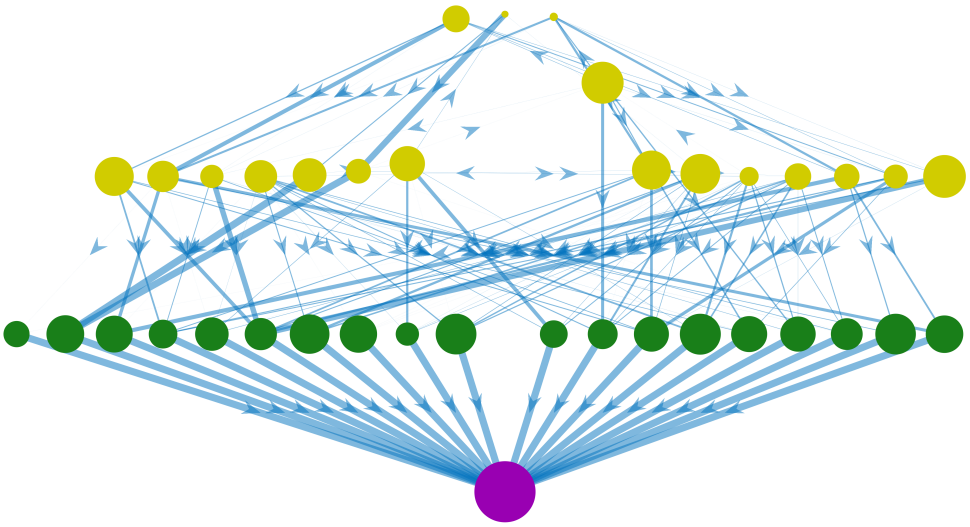

(a) Vertical position proportional to prey-averaged trophic level.

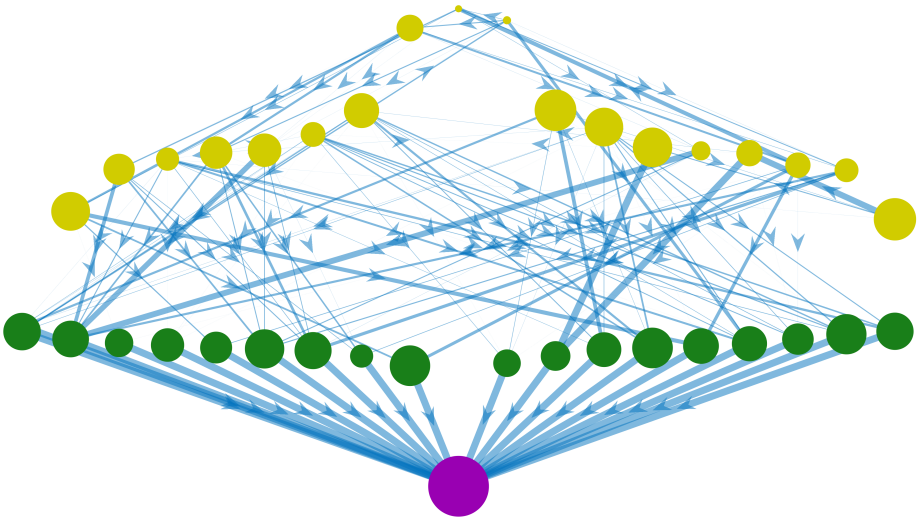

(b) Vertical position proportional to log(*bodysize*).

Figure 3: Final food web for allometric simulation:
- Colour: purple for the resource, green for Basal, yellow for Intermediate. Note: Top species do not appear in this ensemble.
- Size of nodes proportional to the logarithm of biomass.
- Thickness of feeding links proportional to predatory effort. Arrows show direction of predator to prey.

Property	Allometric	Standard $\lambda = 0.3$	Standard $\lambda = 0.1$
Diversity (inc. resource)	44.376 ± 11.004	61.688 ± 6.134	39.242 ± 4.338
Mean population (not inc. resource)	459.419 ± 179.191	1220.559 ± 125.089	1709.078 ± 207.899
Fraction of basal species	0.506 ± 0.072	0.137 ± 0.013	0.211 ± 0.026
Fraction of intermediate species	0.459 ± 0.097	0.863 ± 0.013	0.789 ± 0.026
Fraction of top species	0.035 ± 0.029	0.000 ± 0.000	0.000 ± 0.002
Link density (L/S) inc. resource	3.082 ± 0.377	2.565 ± 0.167	2.118 ± 0.133
Connectance ($2L/(S(S-1))$) inc. resource	0.154 ± 0.037	0.086 ± 0.008	0.113 ± 0.015
Mean shortest-chain trophic level	1.542 ± 0.104	2.653 ± 0.060	2.086 ± 0.046
Maximum shortest-chain trophic level	2.840 ± 0.298	5.093 ± 0.179	3.962 ± 0.126
Mean prey-averaged trophic level	1.583 ± 0.107	2.723 ± 0.062	2.101 ± 0.047
Maximum prey-averaged trophic level	3.137 ± 0.344	5.272 ± 0.235	4.016 ± 0.030
Mean trait overlap on first trophic level	0.512 ± 0.058	0.402 ± 0.047	0.421 ± 0.053
Mean trait overlap on second trophic level	0.316 ± 0.093	0.257 ± 0.045	0.258 ± 0.056
Mean trait overlap on third trophic level	0.296 ± 0.177	0.241 ± 0.062	0.242 ± 0.087
Fraction of omnivorous species	0.101 ± 0.032	0.333 ± 0.055	0.225 ± 0.054
Mean local clustering coefficient (inc. resource)	0.041 ± 0.028	0.038 ± 0.016	0.040 ± 0.021
Mean local clustering coefficient (not inc. resource)	0.042 ± 0.029	0.039 ± 0.017	0.041 ± 0.022
Global clustering coefficient	0.029 ± 0.019	0.038 ± 0.017	0.040 ± 0.021

Table 1: Properties averaged over the final 10,000 evolutionary timesteps of 100 simulations, ± one standard deviation.

3.2. Community properties

To further elucidate the influence of allometry in ecosystem maintenance, we perform 100 simulations of the allometric model, and 100 simulations each of the original non-allometric model (hereafter referred to as "standard model") with two different parameter choices. This version was previously studied in detail [AMG19a], with the only subsequent change being the alterations to the operation of the foraging loop discussed in Section 2. In the allometric simulations the ecological efficiency control parameter λ has been increased from 0.1 to 0.3, and as it is not obvious what parameters for the standard model would best give a comparable control simulation, we perform two sets of simulations: one with $\lambda = 0.3$ and one with λ remaining at 0.1 as in previous experiments.

In Table 1 we compare properties averaged over the final 10,000 evolutionary timesteps of all 100 simulations for each version of the model. When the ecological efficiency parameter is the same ($\lambda = 0.3$), the differences in the model equations due to the inclusion of allometric effects have resulted in significantly reduced diversity, but this can also be achieved by reducing the parameter to 0.1. However, compared to both smaller and larger food webs constructed by the standard model, allometry results in increased connectance, link density and overlap of traits on each trophic level. The decrease in average population is to be expected since body-sizes greater than one necessarily mean that all species now have populations less than their total biomass, which is equivalent to population in the standard model.

There is a much greater fraction of basal species in the allometric simulations (an overestimate compared to empirical data, for example Table 3 in [CHM98]), and all measures of average trophic level are reduced. Due to the body-size kernel influencing predation score (equation (3)), being an effective higher-level predator now requires a larger body-size, resulting in lower populations for the same biomass. This will also contribute to lower average trophic levels, as it is more difficult for higher-level species to prosper. In turn, this ultimately limits the overall diversity, as only finitely-many basal species with a minimum population size can compete for the limited resource. As with the standard model, the number of trophic levels could likely be raised by sufficiently increasing the resource biomass or ecological efficiency parameters. A further possibility is that a much longer simulation may be needed to construct complex networks featuring higher trophic levels, as this now requires that a foundation of prey species are available at the optimal lower body-size *and* a sufficiently large-bodied predator has evolved who could establish the next level.

The fraction of omnivory is significantly reduced but not eliminated, and there is now a non-zero proportion of top species who have no predators. These two facts suggest that the use of body-size has granted additional structure and assembled a food web with a clearer hierarchy. Although food web complexity is desirable, this does improve upon the arbitrary nature of the species in the standard Webworld model where species could occupy *any* trophic position

Species type	**Allometric**	**Standard** $\lambda = 0.3$	**Standard** $\lambda = 0.1$
Basal	548	599	905
Intermediate	1551	2312	4259
Top	886	8	230

Table 2: Average lifespans for Basal, Intermediate, and Top species

Property	**Allometric**	**Standard** $\lambda = 0.3$	**Standard** $\lambda = 0.1$
Species deletion stability	0.481 ± 0.171	0.436 ± 0.117	0.516 ± 0.172
Mean fraction of secondary extinctions	0.030 ± 0.018	0.026 ± 0.010	0.031 ± 0.012
Robustness to random species deletion (10 repeats)	0.320 ± 0.042	0.271 ± 0.022	0.284 ± 0.023
Robustness to most-connected species deletion	0.149 ± 0.051	0.183 ± 0.028	0.186 ± 0.045
Robustness to least-connected species deletion	0.362 ± 0.052	0.312 ± 0.043	0.354 ± 0.041
Robustness to most-connected (non-basal) species deletion	0.289 ± 0.061	0.098 ± 0.025	0.124 ± 0.026
Robustness to least-connected (non-basal) species deletion	0.318 ± 0.065	0.118 ± 0.026	0.156 ± 0.033

Table 3: Stability properties averaged over the final 100 evolutionary timesteps, ± one standard deviation.

and role entirely on the basis of what other species happened to be present.

Next, we compare the average evolutionary lifespans of species during the 300 simulations, meaning how many evolutionary timesteps a species persists before going extinct or arriving at the end of the simulation. This was 760 evolutionary timesteps for the allometric simulations, 1505 for the standard model with $\lambda = 0.3$, and 2148 for the standard model with $\lambda = 0.1$. To see why this is the case, in Table 2, we give a breakdown across the basal, intermediate, and top-species classifications. The role of a species is determined by which of these three it was most often over its lifetime, sampled at the beginning of every evolutionary timestep. Thus, in the allometric model the lower average lifespan is because such a large fraction of the species are basal (Table 1) and this trophic role is highly competitive in all scenarios (Table 2).

Table 3 shows several measures of stability, measured over the final 100 timesteps of each simulation. Species deletion stability is the fraction of species who can be individually removed without causing further extinctions, and we also measure the average number of additional extinctions which are caused, if any. By this measure, smaller networks show slightly greater stability. Community robustness measures the fraction of the food web that must be manually removed before at least 50% of all species have gone extinct as a result of both the artificial deletions and any resulting secondary extinctions, as we iterate the ecological loop once between each manual deletion. To choose the order of species that are removed, we average the results from ten random sequences, and compare this to targeting either the most-connected or the least-connected species possible. Unsurprisingly, sequentially removing species with more prey or predator links has a greater impact on the food web in all scenarios (Table 3). The allometric model constructs food webs that appear slightly more robust against random extinction sequences, in agreement with other models [KGD09], but which are more vulnerable to the most-connected species being removed. However, if we restrict our attention to only removing non-basal species, the allometric simulations gain a significant advantage over the standard models in this regard as well.

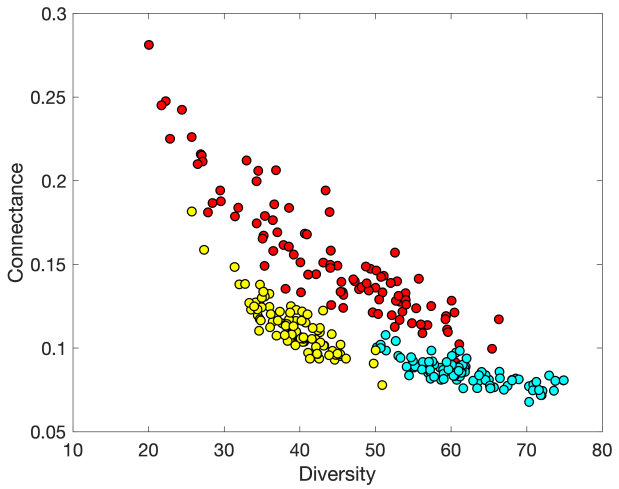

(a) Connectance vs. Diversity

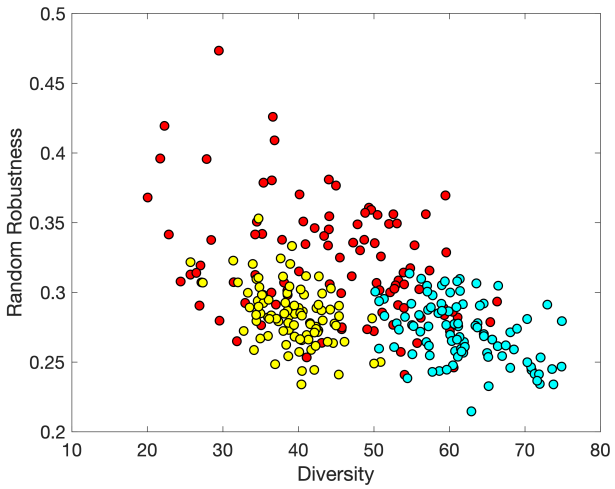

(b) Robustness vs. Diversity

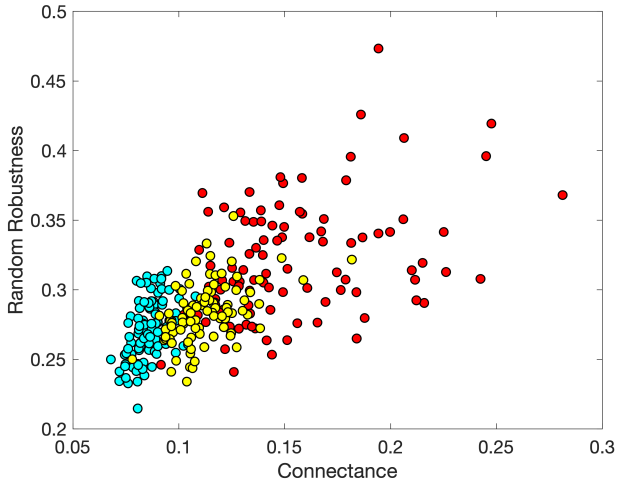

(c) Robustness vs. Connectance

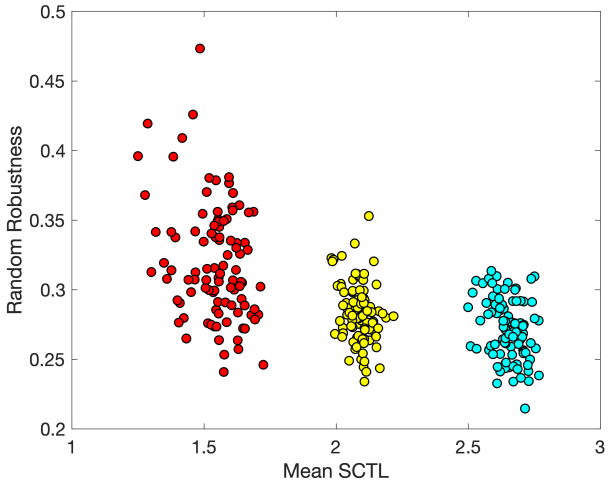

(d) Robustness vs. Mean SCTL

Figure 4: Scatter graphs of individual food web stability-complexity properties:
Red = Allometric
Cyan = Standard model ($\lambda = 0.3$)
Yellow = Standard model ($\lambda = 0.1$)

Figure 4 illustrates some properties of the individual simulations. As we can see from Figure 4(a), the allometric models can construct food webs with a much broader range of sizes than the standard model with a given parameter set. Across all sizes, the networks have increased complexity in the form of connectance within the network (Figure 4(a)), and yield potentially improved robustness throughout this range compared to the standard model (Figure 4(b)). Complexity as food chain lengths are clearly restricted, and thus so are the mean trophic levels (Figure 4(d)), which may be an enabling factor of the improved stability. As in our previous investigations of this model [AMG19a], and in agreement with others [DMW02], there is a clear link between connectance and stability (Figure 4(c)). Interesting, the allometric model is both able to recover this pattern with only a single parameter set, and improve the robustness across the range of network sizes. Thus we uncover some evidence that modelling allometric effects allows more robust food webs that can achieve high diversity by strongly restricting food chains lengths and encouraging multiple feeding links per species. Further plots show no relationship between robustness and the prevalence of omnivory, with the significantly reduced omnivory in the allometric model indicating that species are predating upon multiple prey at the same lower trophic level. If this benefits stability, it would accord with suggested positive relationships between stability and more general ecosystem redundancy [QHM05a].

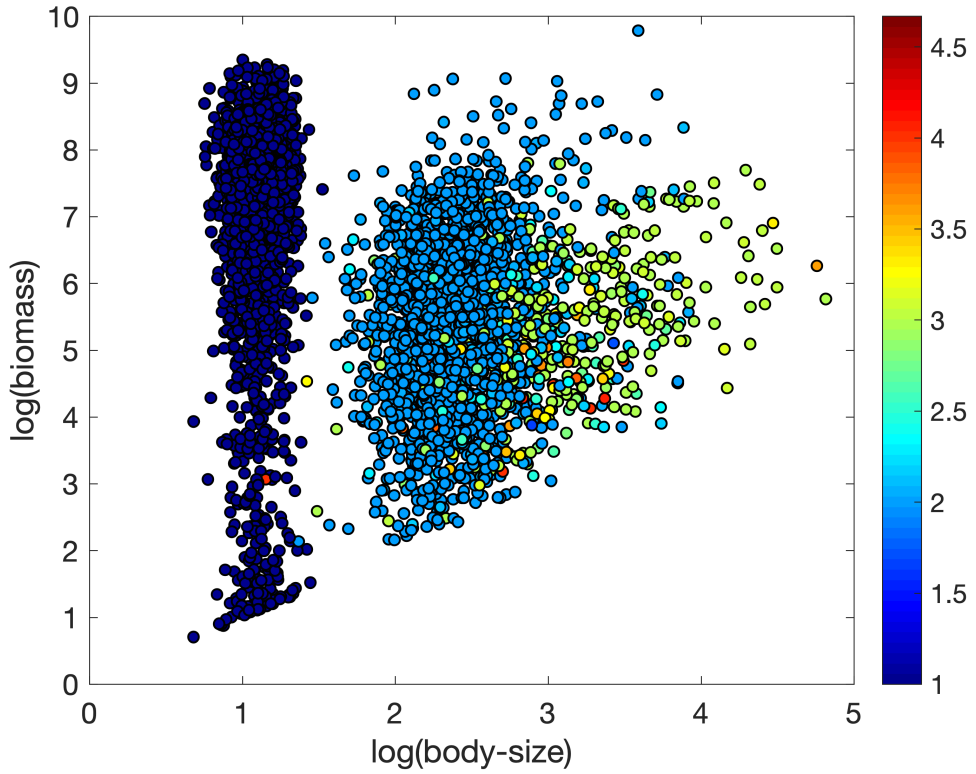

Figure 5: Biomass against body-size for the 100 final allometric simulation food webs (coloured by prey-averaged trophic level)

3.3. Body-size and feeding relationships in the final allometric ensembles

Across the 100 final communities assembled by the allometric version of the model, we have 4421 non-resource species. In the final food webs there were 12,000 realised predator-prey relationships (aside from feeding on the resource), of which 11,444 involved a predator with a larger body-size than its smaller prey. Thus for these simulations, 95.4 % of trophic relationships are between larger predators and smaller prey (ranging from 71.0 % to 100 % of relationships in individual communities), in reasonable agreement with empirical data and structuring the model webs without enforcing a strict hierarchy.

In Figure 5, we illustrate the relationship between biomass and body-size (with nodes coloured by prey-averaged trophic level) for the species across these food webs. Separation of body-sizes into distinct trophic bands, and the lack of dependence between biomass and body-size on a log-log scale are similar to results obtained from other models, particularly a large Population-Dynamical Matching Model community constructed to investigate size-structuring in fishery ecosystems [FFS+13].

3.4. Effects of deleting a single species

Previous researchers have found the number of resulting secondary extinctions when a species is artificially removed from the network to be correlated with its connectedness in the food web [QHM05a]. Here we test whether body-size might be used to predict a species' role in food web stability. At the end of 500,000 evolutionary timesteps in each of the 100 allometric simulations, we recorded the impact of removing each species in isolation and then iterating the population dynamics. The largest secondary extinction wave observed (in both absolute and relative terms) was a loss of 21 species due to deleting a species on the third trophic level with 34 prey and zero predators, from a food web of 52 species (thus, 41.2% of remaining species also perished).

In Figure 6 we show the mean, minimum and maximum fractional extinction events against the following properties of the deleted species: number of prey, number of predators, combined number of prey and predators (i.e. connectedness or degree of the species in network terminology), body-size (grouped in intervals of width 1), and population size (grouped in intervals of width 50). The correlation coefficients of these properties are given for both the allometric

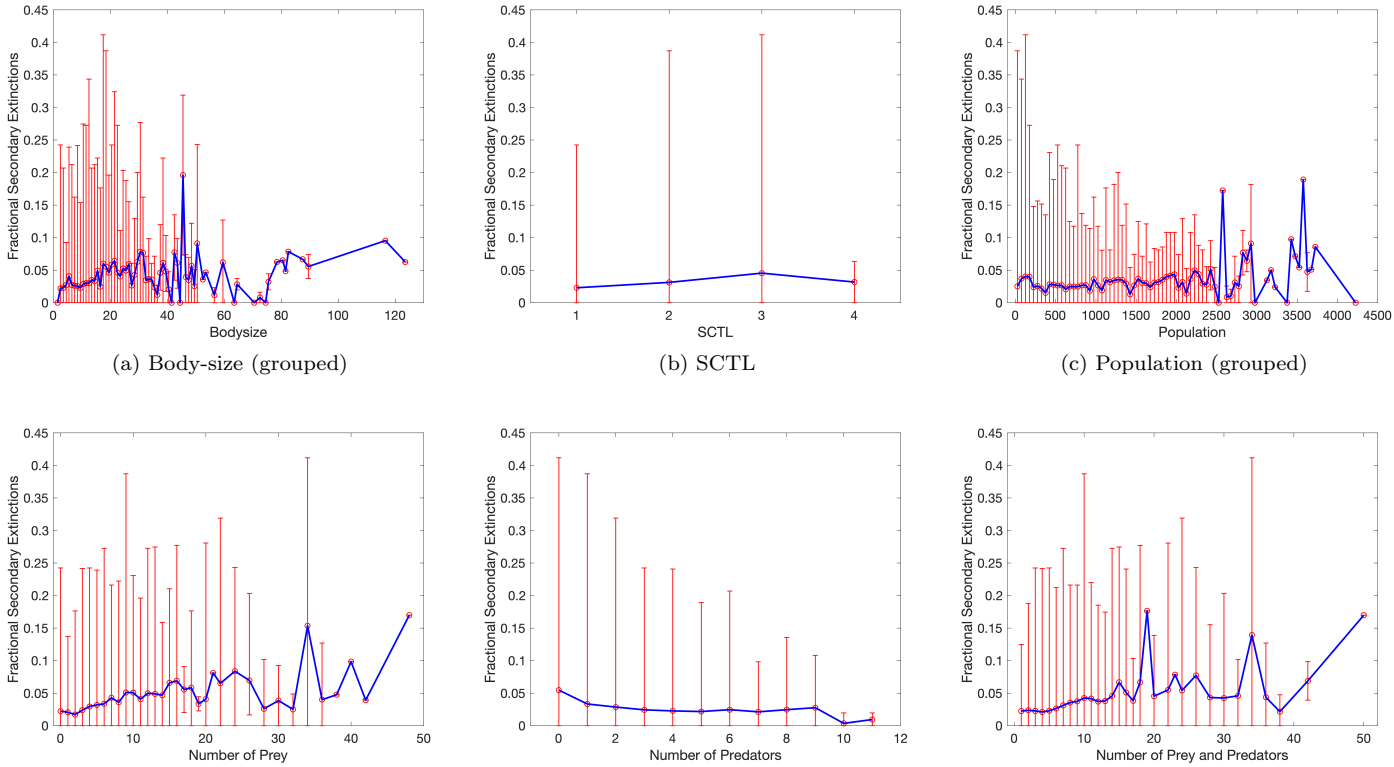

(a) Body-size (grouped) (b) SCTL (c) Population (grouped)

(d) Number of Prey (e) Number of Predators (f) Number of Prey and Predators

Figure 6: Relationship between mean fractional secondary extinctions and selected properties in the final allometric communities. Error bars (red) indicate the range of secondary extinctions.

and standard models in Table 4.

As we see from Table 4, none of the tested properties demonstrated a strong correlation with the fraction of secondary extinctions in the allometric model, and we find no evidence that body-size in particular is a reliable indicator of a species' contribution to stability. There is some evidence of top-down effects in the food webs, with the removal of the rarer species on the third trophic level with small populations, and many prey (one species had 48 prey) being more likely to provoke larger extinction waves (Figure 6(b-d)). However, note two effects of incorporating allometry compared to the standard model: the moderate positive correlation between population and secondary extinctions that exists in the standard model disappears (this remains true when we consider biomass instead for the allometric simulations, so it is not solely due to disentangling population size from biomass); and a weak positive correlation with the number of prey emerges that was not present prior. Previous researchers have found "no clear relationship with complexity" but a correlation between extinctions and the number of links (i.e. predators and prey) of the deleted species [QHM05a], which we recover weakly when allometric effects are included.

Property	**Allometric**	**Standard** $\lambda = 0.3$	**Standard** $\lambda = 0.1$
Body-size	0.170	-	-
Shortest-chain trophic level	0.148	-0.254	-0.285
Population	0.037	0.414	0.494
Biomass	0.098	0.414	0.494
Number of prey	0.237	-0.034	-0.005
Number of predators	-0.112	-0.027	0.194
Number of predators and prey	0.212	-0.038	0.069

Table 4: Correlation coefficients of fractional secondary extinctions against species properties

3.5. Does the final trophic level match that of ancestor species?

To determine if allometric scaling causes the evolutionary branches of species to be more likely to stratify by trophic level early in the simulation, we calculate a new quantity called the trophic matching index. Every 1000 evolutionary timesteps, this measures the a-posteriori probability that a species from the final ensemble has the same shortest-chain trophic level as its ancestor species which exist at that particular timestep. In addition, we calculate the average difference in shortest-chain trophic level between the final species and their existing ancestors at that time. Both quantities are averaged over the 100 simulations for each model and illustrated in Figure 7(a) and (b) respectively.

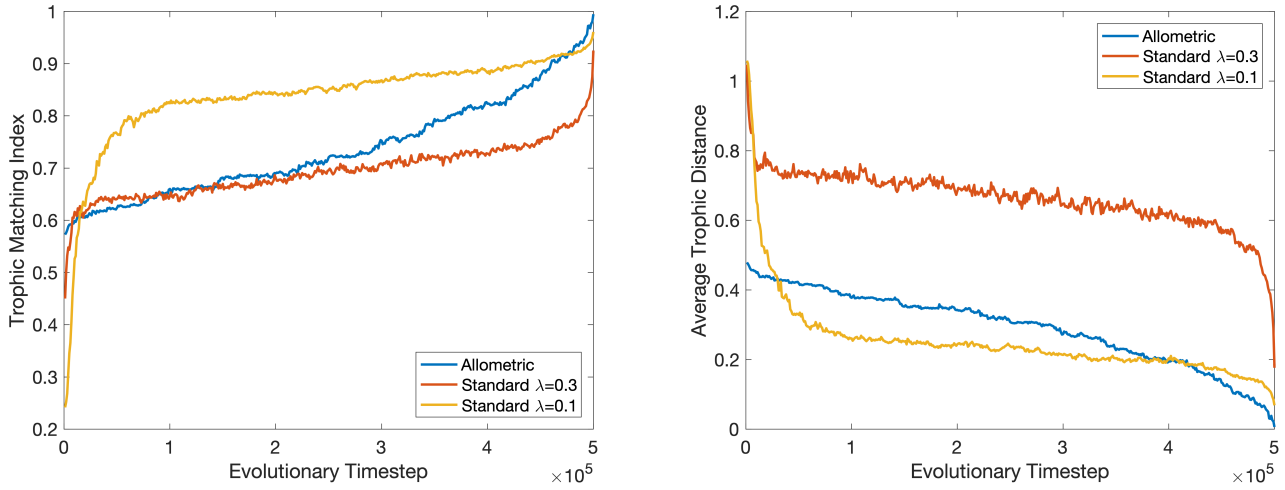

(a) Fraction of current species whose trophic level matches that of their descendants in the final food web

(b) Average difference in trophic level between current species and their descendants in the final food web

Figure 7: Trophic history

Surprisingly, the allometric model does not have the greatest conformity over time, with this instead being maintained by the version that produces the smallest food webs - the standard model, with $\lambda = 0.1$. While the allometric model is very similar in its likelihood of matching exactly with ancestor species to the standard model with $\lambda = 0.3$ (Figure 7(a)), this model has far greater typical differences in trophic level (Figure 7(b)) due to its larger food webs with significantly higher average trophic levels. As most species in the allometric model are on the first or second trophic levels, the potential disparity is limited, and this may be why the matching index does not significantly decrease during the initial 10,000 evolutionary timesteps where the standard model is particularly turbulent, rapidly exploring many unstable arrangements of food chains.

4. Multi-patch meta-community simulations

In this section, we extend the model to a spatial grid of 3×3 patches, where local populations can feed and reproduce in their local environments and then migrate to adjacent patches during step (iii) of the ecological loop. We begin with one unique resource in each of the nine patches, and a single initial non-resource species in patch $(1, 1)$, then the metacommunities assemble over simulations of 110,000 evolutionary timesteps. Two regimes for population movement are compared: in both cases, it is adaptive in response to poor local conditions - whether the effects are due to predation, competition, or a lack of suitable food. In one scenario (henceforth referred to as the "allometric movement" case) movement is also scaled by body-size so that large species are able to move faster. These were described in Section 2.2, equations (9) and (10) for the allometric and non-allometric movement cases respectively.

The time-series of selected local and global properties are illustrated in Figures 8-12. Overall diversity is very similar across both simulations (Figure 8), despite a contrast in the evolution of species with disparate body-sizes (Figures 11-12). Local diversity is greatly reduced in comparison to the individual food web analysed in Section 3.1 with the same parameters as one of these patches, as many more evolutionary timesteps would be required to (on average) subject each of the nine patches to an equivalent 500,000 mutation events. In both simulations, the average (shortest-chain) trophic level in a patch, averaged across all nine patches, remains very close to 1.6 after the first 10,000 evolutionary timesteps. The maximum SCTL achieved, averaged across all patches, is around 3, whilst the overall maximum is typically 4 but occasionally reaches 5 in the first half of the simulations, or drops to 3 in the case of allometric movement (Figures 9-10). Average body-sizes across the metacommunities (Figure 12) are not too dissimilar from the single patch simulation (Figure 1(d)), although they are slightly lower. However this is an expected consequence of the lower local diversity and that the availability of nine distinct resources incentivises a greater number of basal species at the beginning of the simulation compared to a single patch simulation.

The simulation with non-allometric movement was slower to produce species with significantly larger body-sizes (Figure 11), whilst growing in diversity more rapidly. Similarly, towards the end of this simulation diversity rises considerably as average body-size plateaus and the much larger species (body-size greater than 25) die off. However, this does not correlate to a decrease in trophic levels, so this evolutionary branch may have consisted of poorly-adapted large species occupying low trophic levels. As above, we note that multi-patch models may favour a larger proportion of basal species who find one of the nine resources that they can feed on dependably even if they lack the optimal body-size. Examining individual patches reveals that the surge of large-body-size species around 60,000 timesteps (Figure 11(b)) that causes the peak in average body-size (Figure 12(b)) takes place largely in patch (2,1) and the neighbouring patch (3,1). However, these large species failed to reach high trophic levels in these patches, and this poor adaptation may have led to their extinction, causing a brief dip in global diversity around 90,000 timesteps (Figure 8(b)). The increased diversity after 100,000 evolutionary timesteps coincides to a burst in species filling an empty intermediate body-size niche between 10 and 18 in patch (3,1). This bolstered the second and third, but not fourth, trophic levels, thus explaining the increase in diversity without a noticeable change in trophic levels or body-size on a global scale.

Finally, we examined the relationship between body-size and the number of patches that the species occupied. This yielded no correlation in either simulation, as the range of species is largely influenced by the choice of migration rules, with this form of adaptive migration tending to assemble metacommunities where a given species occupies very few patches [AMG19b]. In both scenarios an average range of 1.2-1.3 is achieved in the first 20,000 timesteps, as species explore the environment. Subsequently, most species settle in to occupy only one patch with average range remaining under 1.1 for the remainder of both simulations, suggesting a transition from initial "wide" to eventual "tall" strategies.

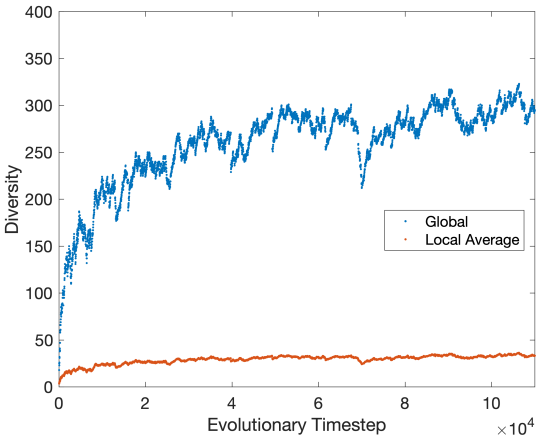

(a) Allometric movement

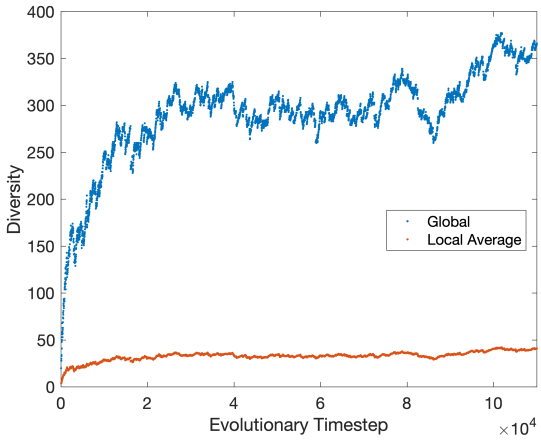

(b) Non-Allometric movement

Figure 8: Time-series of species diversity

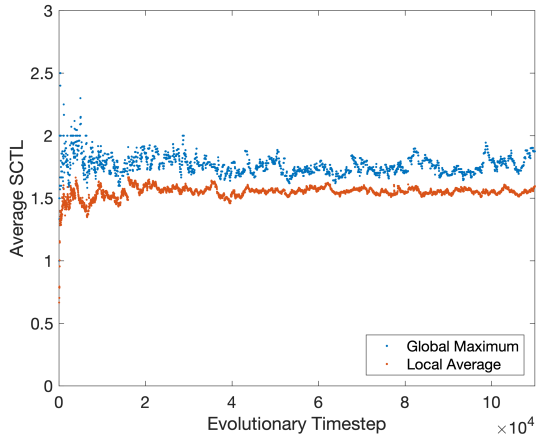

(a) Allometric movement

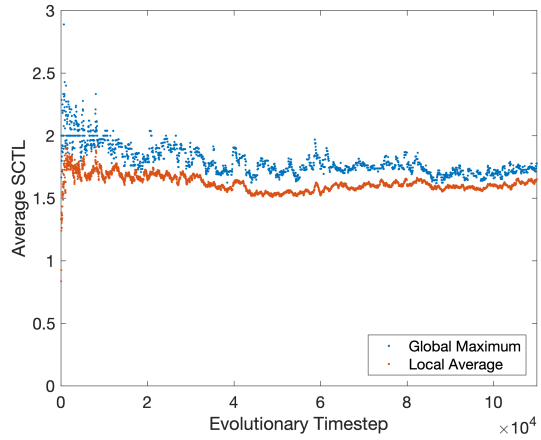

(b) Non-Allometric movement

Figure 9: Time-series of average Shortest-Chain Trophic Level (SCTL) in patches

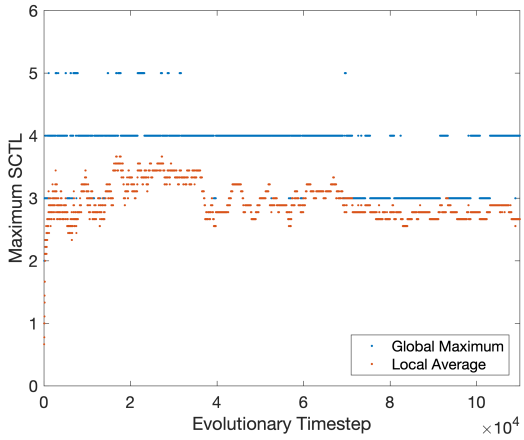

(a) Allometric movement

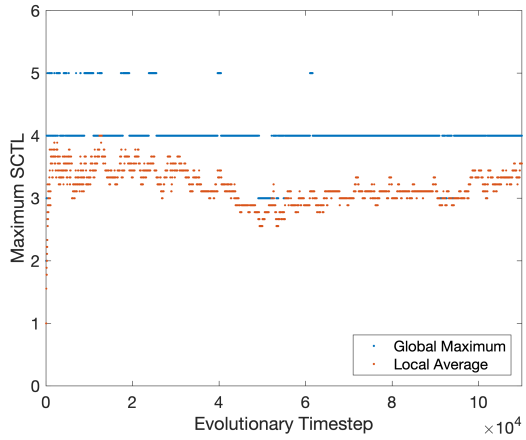

(b) Non-Allometric movement

Figure 10: Time-series of maximum Shortest-Chain Trophic Level (SCTL) in patches

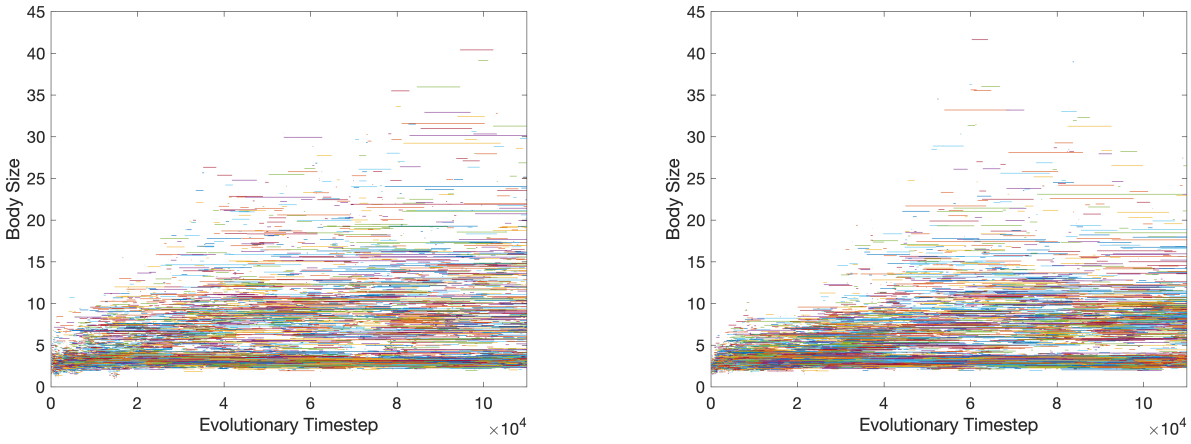

(a) Allometric movement (b) Non-Allometric movement

Figure 11: Existing body-sizes of all species present in simulation

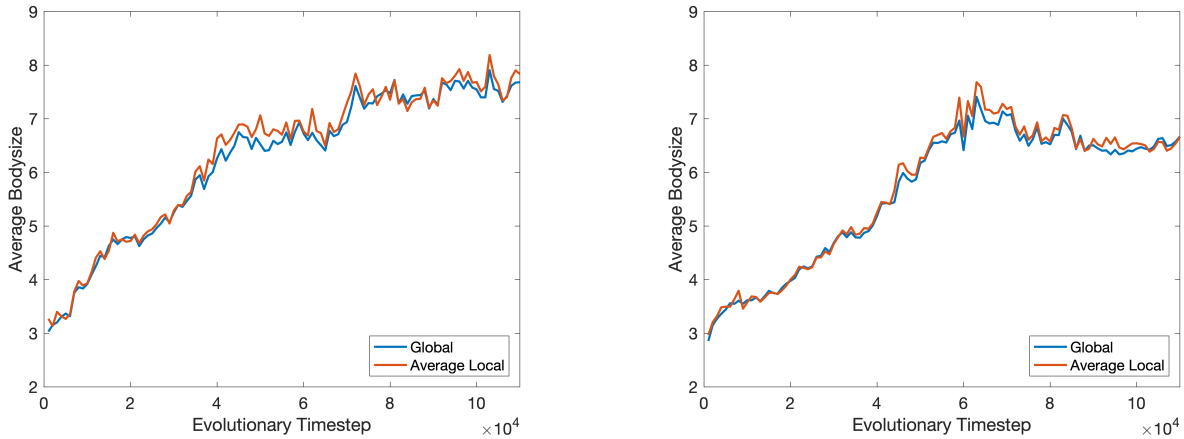

(a) Allometric movement (b) Non-Allometric movement

Figure 12: Average body-size of all species present in simulation

5. Conclusion

Implementing non-strict allometric effects allows the Webworld model to create food webs with reasonable distributions of body-size and biomass by trophic level, and provides a clear framework for diversifying the mortality and ecological efficiency of different species. The body-size of an individual species correlates strongly with trophic position, especially in larger food webs, but proves a poor predictor of the secondary extinctions caused by its removal.

Whilst the trophic role of a given species remains an emergent property of the model, there is now a loose hierarchical structure that curtails the flexibility of species in previous iterations of the model. This comes at the cost of significantly overstimating the proportion of species who feed directly on the resource, even with increased ecological efficiency compared to the original model. However, it is possible that this could be overcome, and a realistic basal-intermediate-top species distribution recovered, by significantly increasing both the resource biomass parameter and the number of evolutionary timesteps of the simulation. Complexity of the assembled networks is maintained as while omnivory is somewhat reduced, a wide range of diversity can be achieved with a greater number of feeding links than larger food webs assembled using the standard model. While allometry reduces the average trophic levels of species, it also enables the persistence of a non-zero fraction of top predators. Due to these changes in the network structure, when compared to food webs of a similar size assembled by the non-allometric version of the model, there are mild benefits to stability against sequential species deletions, in agreement with the patterns previously observed in other kinds of models.

Spatial extensions of the model, utilising adaptive migration rules (whether or not movement itself is influenced by body-size), construct large metacommunities with a variety of body-size distributions in the local food webs. Examining the bodysize time-series provides insight when interpreting bursts of growth and extinction waves that occur in the local food webs. Evidence is found of transition from initial wide strategies as species explore a space, to adaptation to a single local habitat.

[AMG19a] Gavin M Abernethy, Mark McCartney, and David H Glass. The robustness, link-species relationship and network properties of model food webs. *Communications in Nonlinear Science and Numerical Simulation*, 70:20 – 47, 2019.

[AMG19b] Gavin M Abernethy, Mark McCartney, and David H Glass. The role of migration in a spatial extension of the webworld eco-evolutionary model. *Ecological Modelling*, 397:122–140, 2019.

[ARR+15] K. T. Allhoff, D. Ritterskamp, B. C. Rall, B. Drossel, and C. Guill. Evolutionary food web model based on body masses gives realistic networks with permanent species turnover. *Scientific Reports*, 5:10955 EP –, 06 2015.

[BDA17] Lev Bolchoun, Barbara Drossel, and Korinna Theresa Allhoff. Spatial topologies affect local food web structure and diversity in evolutionary metacommunities. *Scientific Reports*, 7(1):1818, 2017.

[BDM+09] Eric L Berlow, Jennifer A Dunne, Neo D Martinez, Philip B Stark, Richard J Williams, and Ulrich Brose. Simple prediction of interaction strengths in complex food webs. *Proceedings of the National Academy of Sciences*, 106(1):187–191, 2009.

[BGA+04] James H. Brown, James F. Gillooly, Andrew P. Allen, Van M. Savage, and Geoffrey B. West. Toward a metabolic theory of ecology. *Ecology*, 85(7):1771–1789, 2004.

[BJB+06] Ulrich Brose, Tomas Jonsson, Eric L. Berlow, Philip H. Warren, Carolin Banasek-Richter, Louis-Félix Bersier, Julia L. Blanchard, Thomas Brey, Stephen R. Carpenter, Marie-France Cattin Blandenier, et al. Consumer-resource body-size relationships in natural food webs. *Ecology*, 87(10):2411–2417, 2006.

[BLLD11] Åke Brännström, Nicolas Loeuille, Michel Loreau, and Ulf Dieckmann. Emergence and maintenance of biodiversity in an evolutionary food-web model. *Theoretical Ecology*, 4(4):467–478, 2011.

[BWM06] Ulrich Brose, Richard J. Williams, and Neo D. Martinez. Allometric scaling enhances stability in complex food webs. *Ecology letters*, 9(11):1228–1236, 2006.

[CHM98] Guido Caldarelli, Paul G. Higgs, and Alan J. McKane. Modelling coevolution in multispecies communities. *Journal of Theoretical Biology*, 193(2):345 – 358, 1998.

[CPYS93] Joel E. Cohen, Stuart L. Pimm, Peter Yodzis, and Joan Saldaña. Body sizes of animal predators and animal prey in food webs. *Journal of Animal Ecology*, 67–78, 1993.

[CRGB08] Björn C. Rall, Christian Guill, and Ulrich Brose. Food-web connectance and predator interference dampen the paradox of enrichment. *Oikos*, 117(2):202–213, 2008.

[DHM01] Barbara Drossel, Paul G. Higgs, and Alan J. McKane. The influence of predator-prey population dynamics on the long-term evolution of food web structure. *Journal of Theoretical Biology*, 208(1):91 – 107, 2001.

[DMQ04] Barbara Drossel, Alan J. McKane, and Christopher Quince. The impact of nonlinear functional responses on the long-term evolution of food web structure. *Journal of Theoretical Biology*, 229(4):539 – 548, 2004.

[DMW02] Jennifer A Dunne, Richard J Williams, and Neo DMartinez. Food-web structure and network theory: the role of connectance and size. *Proceedings of the National Academy of Sciences*, 99(20):12917 – 12922, 2002.

[FFS+13] Tak Fung, Keith D Farnsworth, Samuel Shephard, David G Reid, and Axel G Rossberg. Why the size structure of marine communities can require decades to recover from fishing. *Marine Ecology Progress Series*, 484:155–171, 2013.

[GD08] Christian Guill and Barbara Drossel. Emergence of complexity in evolving niche-model food webs. *Journal of theoretical biology*, 251(1):108–120, 2008.

[HDBG12] Lotta Heckmann, Barbara Drossel, Ulrich Brose, and Christian Guill. Interactive effects of body-size structure and adaptive foraging on food-web stability. *Ecology Letters*, 15(3):243–250, 2012.

[Hem60] Axel M. Hemmingsen. Energy metabolism as related to body size and respiratory surfaces, and its evolution. *Reports of the Steno Memorial Hospital and Nordisk Insulin Laboratorium*, 9:1–110, 1960.

[KGD09] Boris Kartascheff, Christian Guill, and Barbara Drossel. Positive complexity–stability relations in food web models without foraging adaptation. *Journal of theoretical biology*, 259(1):12–23, 2009.

[KHDG10] Boris Kartascheff, Lotta Heckmann, Barbara Drossel, and Christian Guill. Why allometric scaling enhances stability in food web models. *Theoretical Ecology*, 3(3):195–208, 2010.

[LL05] Nicolas Loeuille and Michel Loreau. Evolutionary emergence of size-structured food webs. *Proceedings of the National Academy of Sciences of the United States of America*, 102(16):5761–5766, 2005.

[LM08a] Carlos A. Lugo and Alan J. McKane. The characteristics of species in an evolutionary food web model. *Journal of Theoretical Biology*, 252(4):649 – 661, 2008.

[LM08b] Carlos A. Lugo and Alan J. McKane. The robustness of the webworld model to changes in its structure. *Ecological Complexity*, 5(2):106 – 120, 2008. Current Food-Web Theory.

[McK04] Alan J. McKane. Evolving complex food webs. *The European Physical Journal B - Condensed Matter and Complex Systems*, 38(2):287–295, 2004.

[Pet83] Robert H. Peters. *The Ecological Implications of Body Size*. Cambridge University Press, 1983. Cambridge Books Online.

[Pim82] Stuart L. Pimm *Food Webs*. Springer, 1982.

[QHM02] Christopher Quince, Paul G. Higgs, and Alan J. McKane. Food web structure and the evolution of ecological communities. In Michael Lässig and Angelo Valleriani, editors, *Biological Evolution and Statistical Physics*, volume 585 of *Lecture Notes in Physics*, pages 281–298. Springer Berlin Heidelberg, 2002.

[QHM05a] Christopher Quince, Paul G. Higgs, and Alan J. McKane. Deleting species from model food webs. *Oikos*, 110(2):283–296, 2005.

[QHM05b] Christopher Quince, Paul G. Higgs, and Alan J. McKane. Topological structure and interaction strengths in model food webs. *Ecological Modelling*, 187(4):389 – 412, 2005.

[RJDA18] Tobias Rogge, David Jones, Barbara Drossel, and Korinna T Allhoff. Interplay of spatial dynamics and local adaptation shapes species lifetime distributions and species–area relationships. *Theoretical Ecology*, pages 1–15, 2018.

[WAP10] Richard J Williams, Ananthi Anandanadesan, and Drew Purves. The probabilistic niche model reveals the niche structure and role of body size in a complex food web. *PloS one*, 5(8):e12092, 2010.

[WL87] Philip H. Warren and John H. Lawton. Invertebrate predator-prey body size relationships: an explanation for upper triangular food webs and patterns in food web structure? *Oecologia*, 74(2):231–235, 1987.

[WM00] Richard J. Williams and Neo D. Martinez. Simple rules yield complex food webs. *Nature*, 404(6774):180–183, 03 2000.

[WS03] Craig R. White and Roger S. Seymour. Mammalian basal metabolic rate is proportional to body mass 2/3. *Proceedings of the National Academy of Sciences*, 100(7):4046–4049, 2003.

[YI92] Peter Yodzis and Stuart Innes. Body size and consumer-resource dynamics. *American Naturalist*, pages 1151–1175, 1992.